Reconnection With Magnetic Flux Pileup at the Interface of Converging Jets at the Magnetopause

M. Øieroset, T. D. Phan, J. F. Drake, J. P. Eastwood, S. A. Fuselier, R. J. Strangeway, C. Haggerty, M. A. Shay, M. Oka, S. Wang, et al.

HAL Id: insu-03674459
https://insu.hal.science/insu-03674459

Submitted on 20 May 2022

Geophysical Research Letters

Key Points:
- Magnetic flux pileup observed upstream of reconnecting current sheet at the interface of converging reconnection jets
- Magnetic flux pileup was accompanied by increase in magnetic shear and decrease in $\Delta\beta$, leading to conditions favorable for reconnection
- Magnetic flux pileup leads to enhanced available magnetic energy per particle and strong electron heating

Supporting Information:
- Supporting Information S1
- Figure S1
- Figure S2
- Figure S3
- Figure S4
- Figure S5

Correspondence to:
M. Øieroset,
oieroset@ssl.berkeley.edu

Reconnection With Magnetic Flux Pileup at the Interface of Converging Jets at the Magnetopause

M. Øieroset[1] , T. D. Phan[1] , J. F. Drake[2] , J. P. Eastwood[3] , S. A. Fuselier[4,5] , R. J. Strangeway[6] , C. Haggerty[7] , M. A. Shay[7] , M. Oka[1] , S. Wang[8,9] , L.-J. Chen[8,9] , I. Kacem[10] , B. Lavraud[10] , V. Angelopoulos[6] , J. L. Burch[4] , R. B. Torbert[11] , R. E. Ergun[12] , Y. Khotyaintsev[13] , P. A. Lindqvist[14] , D. J. Gershman[8] , B. L. Giles[8] , C. Pollock[15] , T. E. Moore[8] , C. T. Russell[6] , Y. Saito[16] , L. A. Avanov[8,9] , and W. Paterson[8]

[1]Space Sciences Laboratory, University of California, Berkeley, CA, USA, [2]Department of Physics and the Institute for Physical Science and Technology, University of Maryland, College Park, MD, USA, [3]The Blackett Laboratory, Imperial College London, London, UK, [4]Southwest Research Institute, San Antonio, TX, USA, [5]Department of Physics and Astronomy, University of Texas at San Antonio, San Antonio, TX, USA, [6]Department of Earth, Planetary, and Space Sciences, University of California, Los Angeles, CA, USA, [7]Department of Physics and Astronomy, University of Delaware, Newark, DE, USA, [8]NASA Goddard Space Flight Center, Greenbelt, MD, USA, [9]Department of Astronomy, University of Maryland, College Park, MD, USA, [10]Institut de Recherche en Astrophysique et Planétologie, CNRS, UPS, CNES, Université de Toulouse, Toulouse, France, [11]Institute for the Study of Earth, Oceans, and Space, University of New Hampshire, Durham, NH, USA, [12]LASP, University of Colorado Boulder, Boulder, CO, USA, [13]Swedish Institute of Space Physics, Uppsala, Sweden, [14]Royal Institute of Technology, Stockholm, Sweden, [15]Denali Scientific, Healy, AK, USA, [16]ISAS/JAXA, Sagamihara, Japan

Abstract We report Magnetospheric Multiscale observations of reconnection in a thin current sheet at the interface of interlinked flux tubes carried by converging reconnection jets at Earth's magnetopause. The ion skin depth-scale width of the interface current sheet and the non-frozen-in ions indicate that Magnetospheric Multiscale crossed the reconnection layer near the X-line, through the ion diffusion region. Significant pileup of the reconnecting component of the magnetic field in this and three other events on approach to the interface current sheet was accompanied by an increase in magnetic shear and decrease in $\Delta\beta$, leading to conditions favorable for reconnection at the interface current sheet. The pileup also led to enhanced available magnetic energy per particle and strong electron heating. The observations shed light on the evolution and energy release in 3-D systems with multiple reconnection sites.

Plain Language Summary The Earth and the solar wind magnetic fields interconnect through a process called magnetic reconnection. The newly reconnected magnetic field lines are strongly bent and accelerate particles, similar to a rubber band in a slingshot. In this paper we have used observations from NASA's Magnetospheric MultiScale spacecraft to investigate what happens when two of these slingshot-like magnetic field lines move toward each other and get tangled up. We found that the two bent magnetic field lines tend to orient themselves perpendicular to each other as they become interlinked and stretched, similar to what rubber bands would do. This reorientation allows the interlinked magnetic fields to reconnect again, releasing part of the built-up magnetic energy as strong electron heating. The results are important because they show how interlinked magnetic fields, which occur in many solar and astrophysics contexts, reconnect and produce enhanced electron heating, something that was not understood before.

1. Introduction

Magnetic reconnection is a universal plasma process that converts magnetic energy into particle energy. The reconnection process has been observed in situ by spacecraft at the magnetopause, in the magnetotail, in the magnetosheath, and in the solar wind (e.g., Paschmann et al., 2013). Together, these observations in vastly different regimes show that reconnection occurs for a wide range of plasma conditions. Furthermore, the observations show that the structures and dynamics of reconnection depend strongly on plasma regimes and boundary conditions, such as the strength of the guide field and the degree of asymmetry of the two inflow regions. Thus, for applications of knowledge gained from in situ observations to various regimes

beyond the near Earth space, it is important to understand how reconnection operates under different conditions.

Recently, the Magnetospheric Multiscale (MMS) mission discovered a new region where reconnection takes place, namely, at the interface between converging reconnection jets at the dayside magnetopause (Kacem et al., 2018; Øieroset et al., 2016). Such compressed, thin *interface current sheets* had been observed at the interface of converging jets prior to MMS (Hasegawa et al., 2010; Øieroset et al., 2011, 2014), but only the high-resolution MMS plasma instrumentation resolves the thin current sheets well enough to show that they were reconnecting. The large-scale structures of converging jet events resemble magnetic islands/flux ropes because of the reversal of the normal magnetic field component and the enhancement of the field magnitude near the center of the events. However, density depletion and open magnetic field topology typically seen in such events are inconsistent with closed field magnetic island configurations depicted in Figure 1j (Øieroset et al., 2011, 2016). Furthermore, different electron pitch angle distributions of the converging jets indicate that such structures are not standard flux ropes but rather two interlinked flux tubes where the two converging plasmas are not magnetically connected (Kacem et al., 2018).

The manner in which two tangled flux tubes interact and reconnect is important for understanding the evolution and energy release in 3-D systems with multiple reconnection sites. In this paper we present a new event in which MMS crossed the ion diffusion region in a reconnecting current sheet at the interface of interlinked flux tubes carried by two converging reconnection jets. We also revisit three similar events previously published. We find that magnetic field pileup on approach to the interface current sheet has important consequences for both the occurrence of reconnection and the amount of electron heating in these current sheets.

2. MMS Instrumentation and Orbits

The event was encountered on 10 December 2016 at 04:52–04:55 UT, at 12.1 MLT, when the average inter-spacecraft separation was 6.5 km. We use data from the magnetometer at 128 samples per second (Russell et al., 2014), the fast plasma experiment (Pollock et al., 2016) at 30-ms resolution for electrons and 150 ms for ions, and the electric field instrument at 8,192 samples per second (Torbert et al., 2014).

3. Large-Scale Context

Figures 1a–1i show MMS1 observations, in GSE coordinates, of a thin current sheet at the interface of converging jets at the subsolar magnetopause. A flux rope-like structure was observed between 04:52 and 04:55 UT, with bipolar B_x (Figure 1b) and a large enhancement in the magnetic field magnitude up to 90 nT (Figure 1a). However, as will be explained below, the characteristics of the structure indicate that MMS did not encounter a typical flux rope. The event was observed during an interval of B_Y dominated IMF, with an IMF clock angle near −90° (section S1 in the supporting information; Figure 1k).

Within the structure, there were fast ion flows, mainly in V_{iz}, with speeds up to 200 km/s (Figure 1d). V_{iz} reversed from positive to negative near the center of the structure, at 04:53:32 UT. Coincident with the flow reversal, there were sharp changes in the magnetic field components (Figure 1b), indicating the presence of a thin current sheet at the flow reversal. High-speed flow reversals could indicate converging flows from two X-lines or diverging flows from one X-line (e.g.,Hasegawa et al., 2010; Øieroset et al., 2011). The enhanced magnetic field magnitude at the jet reversal is consistent with the former but not the latter where one would expect a magnetic field strength minimum. Furthermore, four-spacecraft timing analysis (section S2; Schwartz, 1998) indicates that the normal speed of the thin current sheet at 04:53:32 UT was $V_N = -62$ km/s along the current sheet normal $\mathbf{N} = $ GSE(0.628, 0.768, 0.125), that is, $\mathbf{V_N} = $ GSE(−38.9, −47.6, −7.8) km/s. The southward (−z_{GSE}) motion of the current sheet is well illustrated by the order in which the various MMS spacecraft crossed the current sheet along the z direction (section S2). If the thin current sheet was caused (compressed) by converging jets, it would be reasonable to assume that the converging jet structure moved in the same frame of reference as the thin current sheet. Thus, the southward current sheet motion would confirm that the positive-to-negative V_{iz} reversal represents converging rather than diverging jets. Across the thin current sheet there were also significant tangential velocity shears.
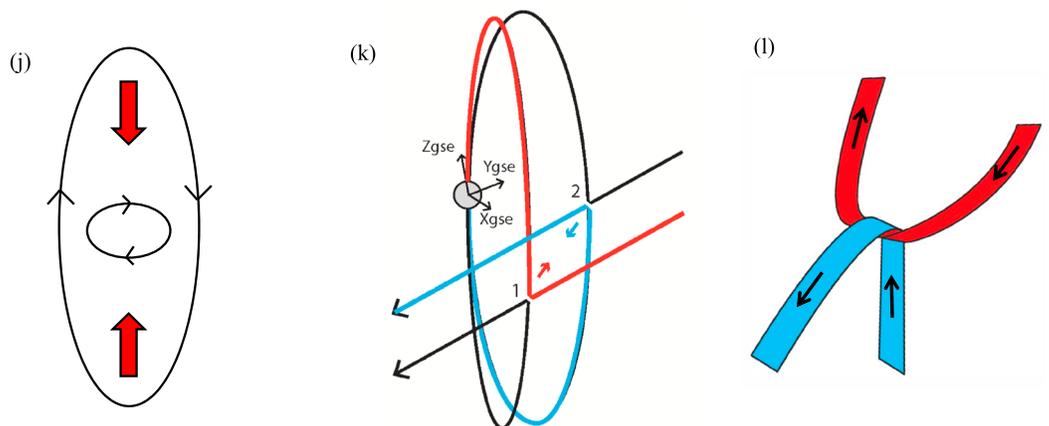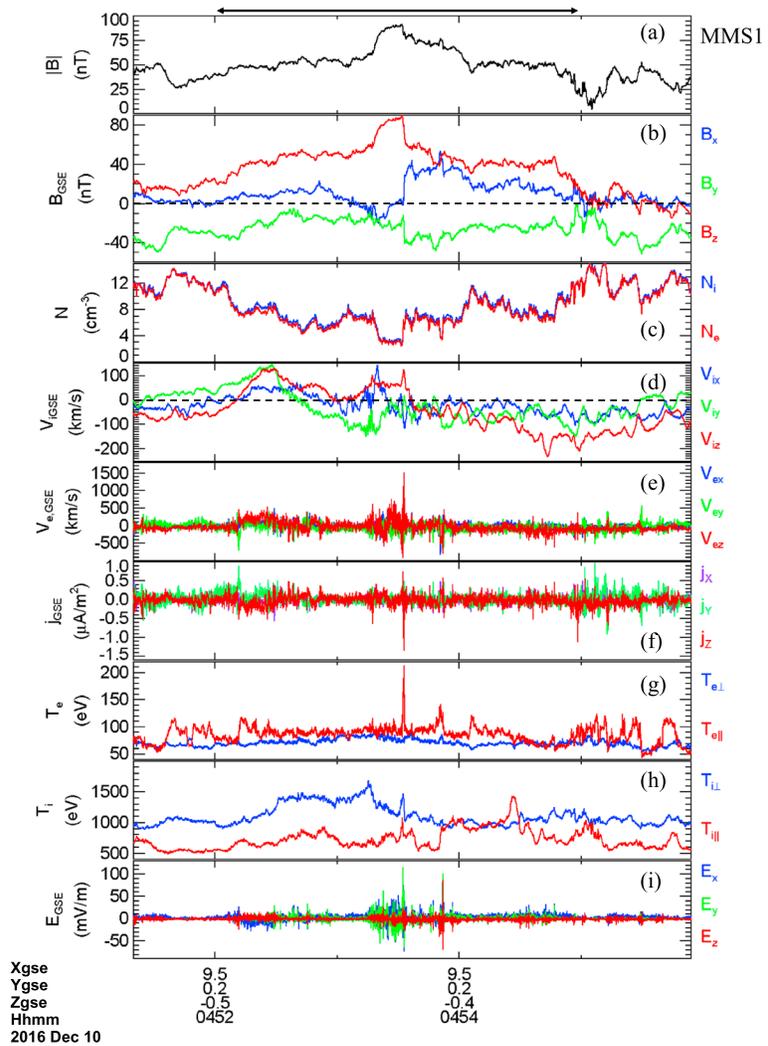
Figure 1. (a–i) MMS1 observations of the large-scale context of the event, in GSE. The interval of enhanced magnetic field and converging jets is marked with the horizontal double arrow. (a, b) Magnetic field magnitude and components, (c) ion and electron densities, (d) ion velocity, (e) electron velocity, (f) current density calculated using plasma data, $\mathbf{j} = eN_e(\mathbf{V_i} - \mathbf{V_e})$, (g) electron temperature, (h) ion temperature, (i) electric field. (j) Two-dimensional cartoon illustrating two converging reconnection jets forming closed magnetic loops, a scenario that is inconsistent with the electron pitch angle data (see Figure 2). (k) Three-dimensional sketch showing how nonsimultaneous reconnection at two locations at the magnetopause (first at "1" and then at "2") can lead to converging plasma jets and interlinked flux tubes. (l) Interlinked flux tubes forming a thin interface current sheet.
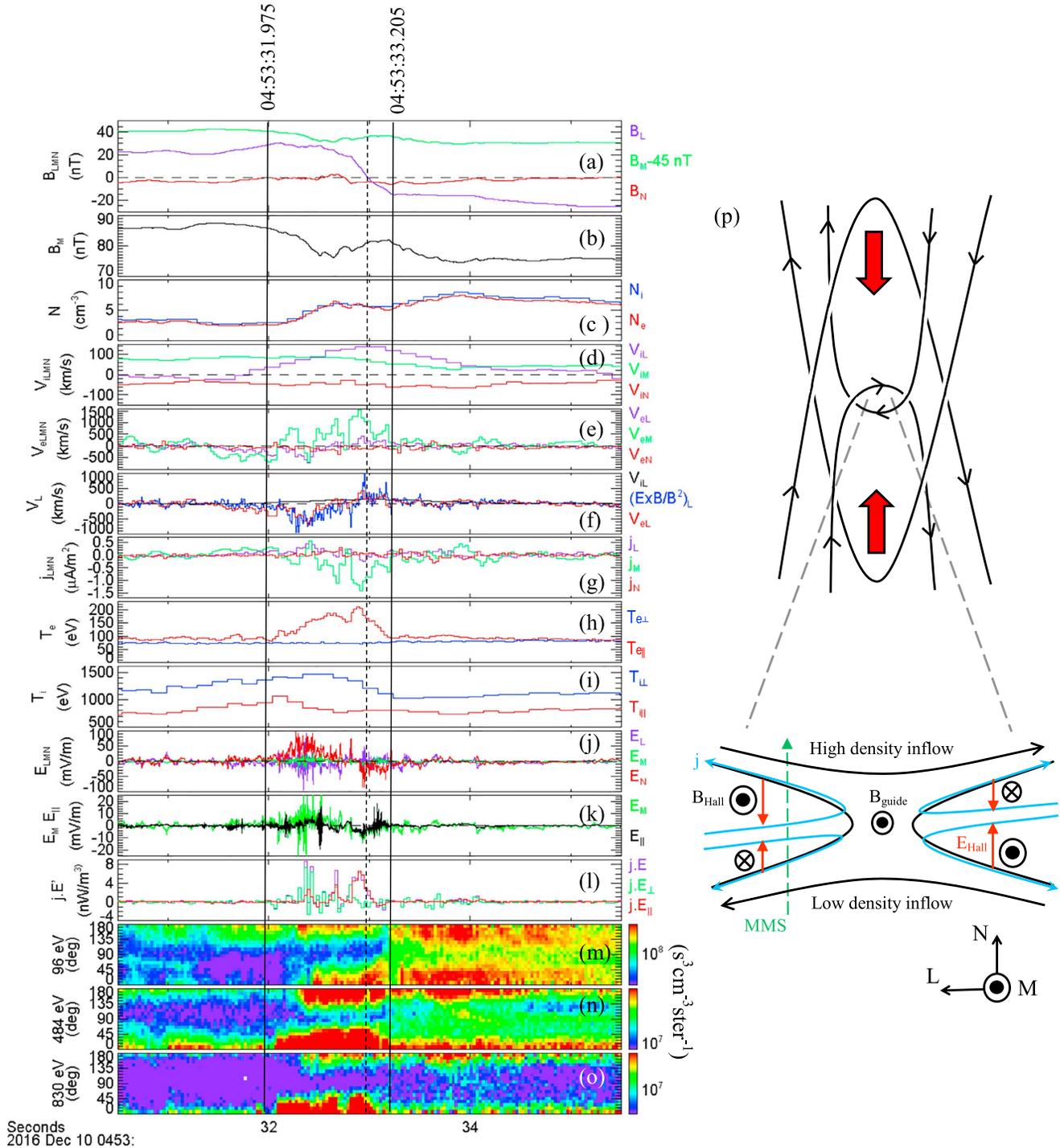
Figure 2. Detailed MMS1 observations of the interface current sheet in LMN, with **L** = GSE(−0.731, 0.530, 0.416), **M** = GSE(0.253, −0.352, 0.894), and **N** = GSE(0.628, 0.768, 0.125). (a) Magnetic field components (B_M shifted by −45 nT), (b) out-of-plane magnetic field B_M, (c) ion and electron densities, (d) ion velocity, (e) electron velocity, (f) V_{iL}, V_{eL}, and $(\mathbf{E} \times \mathbf{B}/B^2)_L$, (g) current density $\mathbf{j} = eN_e (\mathbf{V}_i - \mathbf{V}_e)$, (h) electron temperature, (i) ion temperature, (j) electric field, (k) E_M and $E_{||}$, (l) $\mathbf{j} \cdot \mathbf{E}' = \mathbf{j} \cdot (\mathbf{E} + \mathbf{V}_e \times \mathbf{B})$, (m–o) electron pitch angle spectrograms for 96-, 484-, and 830-eV electrons, (p) conceptual sketch of the 2-D projection of the magnetic field in the interlinked 3-D structure (Figures 1k and 1l) in the L-N plane, with a close-up of the interface current sheet and a possible MMS trajectory. Different energy flux intensities and pitch angle behaviors to the left and right of the current sheet indicate that the two inflow regions are not magnetically connected. The vertical solid lines in (a–o) mark the separatrices (see section S5). The vertical dashed line marks $B_L = 0$.

The electron pitch angle distributions (Figures 2m–2o) were different on the two sides of the thin current sheet. To the left of the current sheet, the 96-eV electrons were predominantly antifield aligned, while the 830-eV electron fluxes were higher along the magnetic field. To the right of the current sheet, both the 96- and the 830-eV electron fluxes were much more intense and were observed both at 0° and 180° pitch angles. These differences indicate that the two converging plasmas were not magnetically connected when they approached each other (see also Kacem et al., 2018; Øieroset et al., 2011), that is, inconsistent with the scenario in Figure 1j. The unconnected converging field lines could eventually tangle up as illustrated in Figures 1k and 1l. Similar scenarios have previously been proposed by Nishida (1989), Hesse et al. (1990), Lee et al. (1993), Otto (1995), Louarn et al. (2004), Cardoso et al. (2013), Perez et al. (2018), and Kacem et al. (2018). The interlinked field line scenario and its association with the observed enhancement/pileup of magnetic field outside the thin current sheet will be discussed in more detail in section 5.

Inside the thin current sheet, marked by the sharp changes in the magnetic field at ~04:53:32 UT, MMS1 observed enhancements in the ion and electron velocities (Figures 1d and 1e), large current densities up to 1.4 μA/m^2 (Figure 1f), ~140-mV/m peak electric field (Figure 1i), and enhanced electron and ion temperatures (Figures 1g and 1h). In the next section we show that the converging reconnection jets created a compressed interface current sheet which itself underwent reconnection.

4. Detailed MMS1 Observations of the Interface Current Sheet

4.1. LMN Coordinate System of Interface Current Sheet

Figure 2 shows a close-up of the interface current sheet in boundary normal (LMN) coordinates, which were determined using a hybrid variance analysis method. The current sheet normal (**N**) direction was obtained using timing analysis on the interface current sheet crossings by the four spacecraft (section S2). The **M** direction is from $\mathbf{L'} \times \mathbf{N}$, where $\mathbf{L'}$ is the direction of maximum variance of the magnetic field (Sonnerup & Cahill, 1967). Finally, $\mathbf{L} = \mathbf{N} \times \mathbf{M}$. The **N** direction from the multispacecraft timing analysis, GSE(0.628, 0.768, 0.125), differs from the direction of the minimum variance of the magnetic field (Sonnerup & Cahill, 1967), GSE(0.705, 0.699, 0.118), by only 6°.

4.2. Plasma and Field Profiles in the Interface Current Sheet

The boundary conditions of the interface current sheet were weakly asymmetric, with a factor of 2 difference in the inflow plasma densities (Figure 2c). The magnetic shear across the current sheet was 37°, that is, the guide field was 3 times the reconnecting magnetic field. The hybrid inflow ion Alfvén speed based on the two inflow densities and magnetic field B_L (Cassak & Shay, 2007) was 274 km/s.

The separatrices, marked by the solid vertical black lines in Figure 2 at 04:53:31.975 and 04:53:33.205 UT, were identified based on the electron distributions (section S5). The crossing duration of the region bounded by the separatrices was ~1.23 s. Using the current sheet propagation speed of ~62 km/s along **N**, the width of the region was ~80 km or 0.8 ion inertial lengths (d_i) where d_i = 103 km based on the hybrid density in the two inflow regions of 5 cm^{-3} (Cassak & Shay, 2007). The thin d_i-scale current sheet suggests that MMS crossed the reconnection layer near the X-line. Indeed, the comparison of the ion and electron perpendicular velocities with the $\mathbf{E} \times \mathbf{B}/B^2$ velocity (section S4) reveals that the ions were not frozen-in, while $V_{e\perp}$ and $\mathbf{E} \times \mathbf{B}/B^2$ showed good overall agreements, except on fine scales. These findings indicate that the spacecraft encountered the ion diffusion region but probably not the electron diffusion region.

Even though the ions were not frozen-in, there were enhanced ion outflows, V_{iL}, inside the current sheet, with peak speed of 130 km/s relative to the external flows (Figure 2d). This outflow speed is substantially lower than the hybrid Alfvén speed of 274 km/s. Interestingly, the enhanced ion flows extended well outside the separatrices, which may be a characteristic of ion dynamics close to the X-line. Together with the negative to positive B_M variation (relative to the guide field; Figure 2b), which is indicative of the Hall magnetic field pattern (Sonnerup, 1979), the $V_{iL} > 0$ jet indicates that MMS crossed the reconnection layer on the left side of the X-line in the reconnection configuration shown in Figure 2p.

Unlike the ion jet, the large electron flows (Figure 2e), high current densities (Figure 2g), large electric fields (Figure 2j), and positive magnetic-to-particle energy conversion in the electron frame of reference, $\mathbf{j} \cdot \mathbf{E'} = \mathbf{j} \cdot (\mathbf{E} + \mathbf{V_e} \times \mathbf{B}$; Figure 2l), were mostly confined to the region between the separatrices. The largest
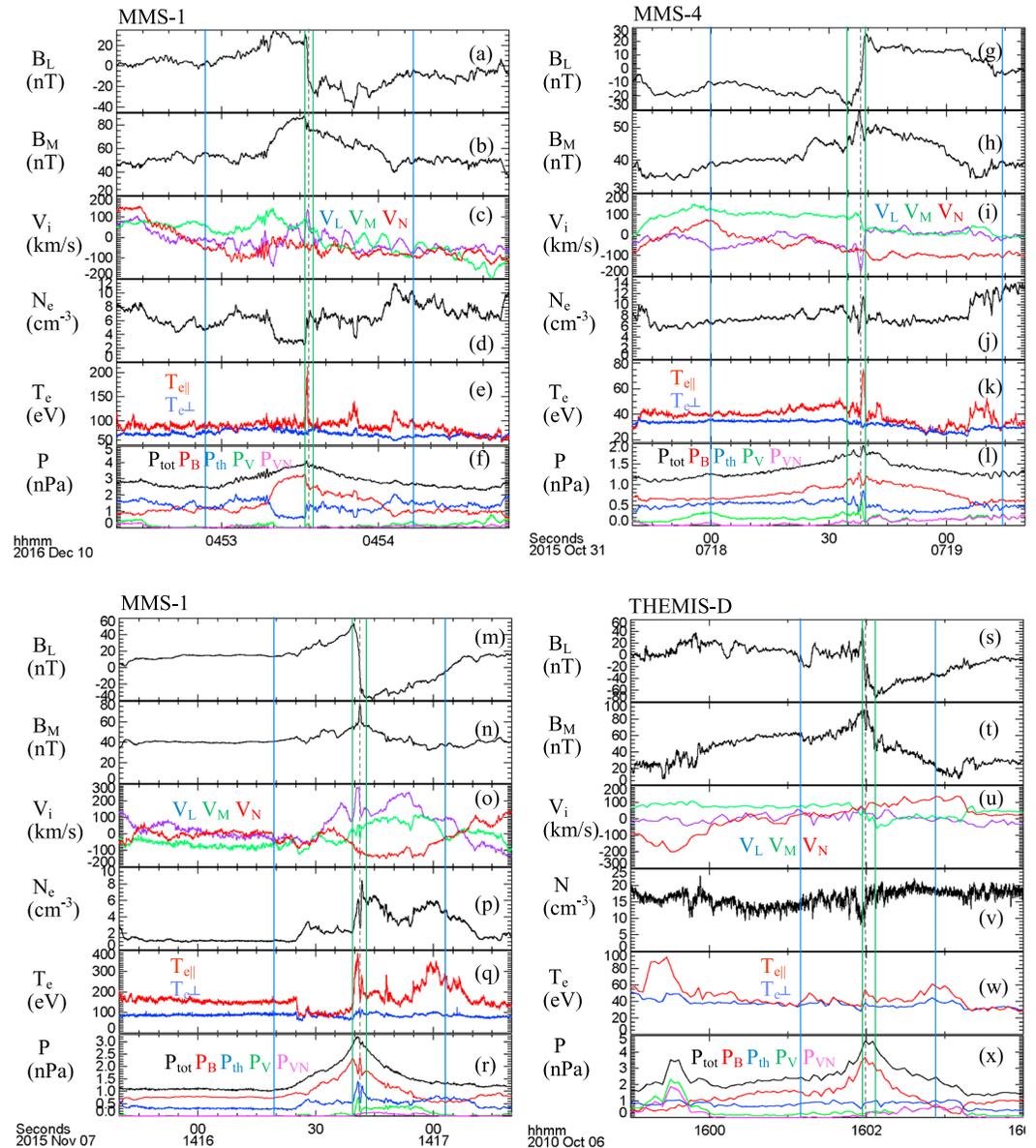
Figure 3. Presence of significant magnetic flux pileup in four reported converging jet events. (a–f) The 10 December 2016 MMS event presented in detail in this paper. (a, b) Reconnecting and out-of-plane component of the magnetic field; (c–e) Vi, electron density, and electron temperature; (f) total, magnetic, thermal, and dynamic pressure based on total V and VN. (g–l) The 31 October 2015 MMS event (Øieroset et al., 2016). The panels are the same as in a–f. (m–r) The 7 November 2015 MMS event (Kacem et al., 2018). The panels are the same as in a–f. (s–x) The 6 October 2010 THEMIS event (Øieroset et al., 2011, 2014). The panels are the same as in a–f. The blue and green vertical lines indicate times of prepileup and postpileup of the magnetic field.

electron bulk velocity and current density were observed in the out-of-plane (M) direction, reaching 1,600 km/s and 1.4 μA/m^2, respectively (Figures 2e and 2g). V_{eL} (Figures 2e and 2f) was bipolar in the current sheet, with $V_{eL} < 0$ (directed toward the X-line and opposing V_{iL}) near the left separatrix and lasting until ~04:53:32.600 UT, followed by $V_{eL} > 0$ (directed away from the X-line). Near the center of the current sheet, the enhanced $\mathbf{j} \cdot (\mathbf{E} + \mathbf{V_e} \times \mathbf{B})$ in the current layer was dominated by j$_{||}$E$_{||}$ (Figure 2l), which is a characteristic of strong guide field reconnection (Genestreti et al., 2017; Phan et al., 2018; Wilder et al., 2017).

The bipolar E_N (Figure 2j) is consistent with the Hall electric field in symmetric reconnection (Shay et al., 1998). The good agreement between V_{eL} and $(\mathbf{E} \times \mathbf{B})_\mathbf{L}$/B^2 (Figure 2f) indicates that the electron outflows were driven predominantly by the dominant E_N and B_M, thus perpendicular to the magnetic field.

Finally, enhancements in the ion temperature and the electron parallel temperature were observed in the reconnection layer (Figures 2h and 2i).

5. Magnetic Field Pileup

We now discuss how the occurrence of reconnection and the strong electron heating in the interface current sheet could be associated with magnetic field pileup in its inflow regions.

Figures 3a–3f display 2 min of observations surrounding the interface current sheet for the event presented above. B_L and B_M increased in magnitude toward the thin current sheet on both sides of the current sheet (Figures 3a and 3b). The accompanying decrease in density (Figure 3d) indicates that the magnetic pileup process was not adiabatic and that the pileup region may be similar to the plasma depletion layer upstream of the Earth's magnetopause during northward IMF, where plasma is squeezed out along piled up magnetic field (e.g., Crooker et al., 1979; Paschmann et al., 1978).

Three previously published events where a thin current sheet appeared at the interface of converging jets are shown in Figures 3g–3x, two observed by MMS (Kacem et al., 2018; Øieroset et al., 2016), and one by THEMIS-D (Øieroset et al., 2011). All four events displayed substantial B_L pileup in the inflow region and enhanced B_M. We now explore the causes and effects of the magnetic field pileup.

5.1. Magnetic Tension and Pressure Balance in the Converging Jet Structure

In all four events, the magnetic field pileup led to enhanced magnetic pressure (Figures 3f, 3l, 3r, and 3x— red curve, labeled P_B) which was only partially compensated for by a decrease in the thermal pressure (blue curve, labeled P_{th}). The total pressure (Figures 3f, 3l, 3r, and 3x, black curves, labeled P_{tot}) here is the sum of magnetic pressure, plasma thermal pressure, and plasma dynamic pressure. Since one would expect the events to roughly be in pressure balance, the nonconstant total pressure with a peak near the center of the structure implies that not all significant pressure terms have been included. We now investigate what that missing force term could be.

Strong driving from the converging plasma jets exceeding the reconnection rate at the interface current sheet could in principle lead to the observed magnetic field pileup. However, the dynamic pressure contribution, based on the total plasma speed (P_V, green) or V_N alone (P_{VN}, pink), was much too small to compensate for the enhanced magnetic pressure, indicating that driving did not play a significant role.

It has previously been shown that an apparent violation of pressure balance across flux transfer events could be due the neglect of the magnetic tension term (e.g., Paschmann et al., 1982). We now consider whether magnetic tension can balance the enhanced pressure in these events as well. Magnetic tension could be significant when magnetic fields from two unconnected X-lines become interlinked (Figures 1k and 1l).

The total pressure enhancement from the edge of the structure to its center was ~1.5 nPa in the 10 December 2016 event (Figure 3f). The enhancement occurred over ~30 s, which corresponds to ~1,800 km using the estimated propagation speed of the structure of 62 km/s. Thus, the total pressure gradient was ~0.8×10^{-15} Pa/m.

To check whether the magnetic tension force of the overall structure could balance the pressure gradient, we approximate the tension term $\frac{1}{\mu_0}(\mathbf{B}\cdot\nabla)\mathbf{B}$ by $\frac{1}{\mu_0}\frac{B^2}{r_C}$, where r_C is the radius of curvature for the magnetic field and $\mathbf{B}$ is the magnetic field at the edge of the structure (before pileup). Equating 0.8×10^{-15} Pa/m to $\frac{1}{\mu_0}\frac{B^2}{r_C}$, and using a prepileup magnetic field value of ~50 nT, $r_C = $ ~2,500 km is obtained. This is comparable to the estimated 1,800-km size of the pressure enhancement from the edge of the structure to its center, indicating that the excess pressure can be balanced by magnetic tension associated with interlinked fields.

It should be noted that the local current density (in a structure with |$\mathbf{B}$| ~ 50 nT) needed to counter a 10^{-15}-Pa/m pressure gradient (assuming force balance) is only 0.02 μA/m^2, which is not detectable.

5.2. Magnetic Field Pileup and the $\Delta\beta$-Magnetic Shear Condition for Reconnection

Magnetic field pileup in the inflow region is not commonly observed in reconnection in space. We now examine a possible reason for the occurrence of magnetic field pileup associated with reconnection in the
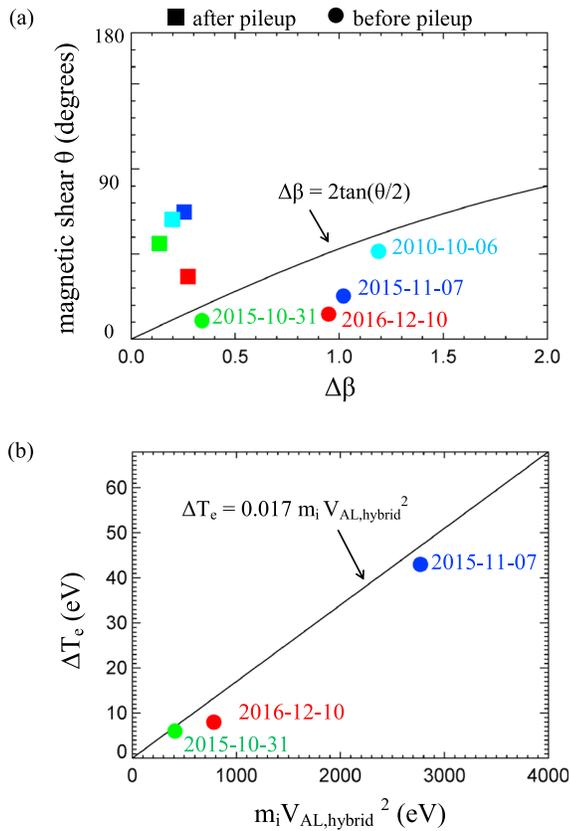
Figure 4. (a) Magnetic shear versus difference in β on the two sides of the interface current sheet, before pileup (circles) and after pileup (squares) for the four events in Figure 3. The theoretical curve from (1) for $L = 1$ is also plotted. (b) Electron heating in a reconnecting current sheet as a function of available magnetic energy per particle immediately upstream. The black line shows the empirical relation from Phan, Shay, et al. (2013) and the circles the three MMS events in Figure 3.

interface current sheet. The analysis below suggests that magnetic flux pileup is required to overcome the suppression of reconnection by diamagnetic drift stabilization (Swisdak et al., 2003, 2010).

For a given magnetic shear θ across a current sheet, reconnection is allowed (suppressed) if $\Delta\beta$, the difference in plasma β in the two inflow regions, satisfies (does not satisfy) the following relation:

$$\Delta\beta < 2(L/\lambda_i)\tan(\theta/2) \tag{1}$$

where L/λ_i is the width of the current sheet in units of ion skin depth λ_i (Swisdak et al., 2010). The relation is shown in Figure 4a for $L/\lambda_i = 1$ (solid curve), which best described solar wind (Phan et al., 2010) and magnetopause reconnection events (Phan, Paschmann, et al., 2013).

Figure 4a also shows the observed $\Delta\beta$ and magnetic shear before (circles) and after (squares) pileup for the four events in Figure 3. The before/after times are marked in Figure 3 with pairs of blue/green vertical lines. In all four events the conditions changed from reconnection being suppressed (i.e., below the curve in Figure 4a) before pileup to reconnection being allowed (above the curve) after pileup. Interestingly, the magnetic field pileup on approach to the center of the structures is associated with both an increase in magnetic shear and a decrease in $\Delta\beta$. These results suggest that magnetic field pileup was necessary for the interface current sheet to reconnect. The increasing magnetic shear, which did not exceed 90° in any of the events, suggests that as field lines tangle up, they tend to rotate to become more perpendicular to each other, as illustrated in Figure 1l.

5.3. Magnetic Field Pileup and Electron Heating

A striking feature of the reconnecting interface current sheet is the large parallel electron temperature relative to the surrounding plasma (Figures 3e, 3k, and 3q). There was no perpendicular electron heating, consistent with previous observations and simulations of strong guide field reconnection (e.g., Phan, Shay, et al., 2013; Shay et al., 2014).

In an earlier statistical study of electron heating in reconnection exhausts at the magnetopause (Phan, Shay, et al., 2013), it was found that the degree of electron heating, ΔT_e, is proportional to the available magnetic energy per particle, $m_i V_{AL}^2$ (see also Haggerty et al., 2015; Shay et al., 2014)

$$\Delta T_e = 0.017\, m_i V_{AL,\text{hybrid}}^2 \tag{2}$$

where m_i is the ion mass and $V_{AL,\text{hybrid}}$ is the hybrid inflow Alfvén speed (Cassak & Shay, 2007) based on the asymmetric inflow magnetic field B_L and densities. This empirical relation is plotted in Figure 4b (black line).

In the 10 December 2016 event the average total electron heating in the current sheet was $\Delta T_e = 1/3(\Delta T_{e||} + 2\Delta T_{e\perp}) \sim 8$ eV. The green vertical lines in Figures 3a–3f mark the edges of the current sheet, which for this event were located outside the separatrices, a characteristic of the diffusion region (Phan et al., 2016). In the 31 October 2015 event, ΔT_e was 6 eV, and in the 7 November 2015 event, it was 43 eV. In the 6 October 2010 THEMIS event electron heating in the current sheet was not resolved. Using the conditions immediately upstream of the interface current sheet, the hybrid inflow Alfvén speed for the three MMS events was 274 km/s for the 10 December 2016 event, 200 km/s for the 31 October 2015 event, and 515 km/s for the 7 November 2015 event. Using these values, the observed electron heating versus the available magnetic energy for the three MMS events (Figure 4b) is in reasonable agreement with the empirical relation (2) for magnetopause reconnection exhaust heating.

Finally, we note that the inflow region has been significantly affected by the magnetic field pileup in these events. In the 10 December 2016 event $|B_L|$ (Figure 3a) increased by at least a factor of 5 (from ~5 to 30 nT and 25 nT) from the prepileup region (blue vertical lines) to the region immediately upstream of the interface current sheet (green vertical lines). At the same time the density decreased. As a result the hybrid inflow Alfvén speed increased by a factor of ~7, from ~40 to ~274 km/s, and the available magnetic energy, $m_i V_{AL}^2$, increased by a factor of 49. In the two other MMS events (Figures 3g–3r) the available magnetic energy increased by a factor of 100 and 49, respectively. Thus, the electron heating in these reconnection events, predicted to be proportional to the available magnetic energy in the inflow regions immediately adjacent to the current sheet, was substantially (50–100 times) higher than it would have been without flux pileup. On the other hand, the degree of electron heating in these three events, as well as their dependence on the available magnetic energy, is similar to magnetopause reconnection events without pileup, suggesting that the electron heating physics associated with flux pileup reconnection is not that different from nonpileup reconnection.

6. Summary

We have presented a new MMS event of reconnection in a thin current sheet at the interface of converging reconnection jets and reexamined three previously reported events. We summarize the main findings here as follows:

1. The ion skin depth-scale width of the interface current sheet and the non-frozen-in ions indicate that MMS crossed the reconnecting interface current sheet near the X-line, in the ion diffusion region.
2. The electron pitch angle distributions indicate that the two converging plasmas were not magnetically linked. The large-scale structure of these converging jet events is therefore not consistent with regular flux ropes. They are more consistent with interlinked flux tubes emanating from two X-lines (Figures 1k and 1l).
3. Magnetic field pileup was observed on both sides of the interface current sheet and was associated with enhanced magnetic pressure that was not balanced by the thermal or dynamic pressure. We revisited three previously published converging jet events and found similar flux pileup in those events. The enhanced magnetic pressure in these events could be balanced by the magnetic tension, that is, the magnetic field pileup arises from the effect of interlinking of the magnetic flux tubes, which may not reconnect at first.
4. The pileup of magnetic flux is associated with an increase in the magnetic shear and a decrease in $\Delta\beta$. This evolution changed the inflow conditions from reconnection being suppressed before pileup to reconnection being allowed after pileup, leading to favorable conditions for reconnection in the interface current sheet.
5. The magnetic field pileup in the inflow region also significantly enhances the available magnetic energy per particle and leads to strong electron heating in the interface current sheet.

These findings reveal interesting reconnection onset physics associated with tangled up flux tubes, a phenomenon that should be common in multiple X-line reconnection scenarios with strong guide fields. At the magnetopause these structures could play a role in flux transfer event formation when the IMF has a significant east-west component, as seen in some global MHD simulations (e.g., Cardoso et al., 2013; Perez et al., 2018).

References

Cardoso, F. R., Gonzalez, W. D., Sibeck, D. G., Kuznetsova, M., & Koga, D. (2013). Magnetopause reconnection and interlinked flux tubes. *Annales de Geophysique*, *31*(10), 1853–1866. https://doi.org/10.5194/angeo-31-1853-2013

Cassak, P. A., & Shay, M. A. (2007). Scaling of asymmetric magnetic reconnection: General theory and collisional simulations. *Physics of Plasmas*, *14*(10), 102114. https://doi.org/10.1063/1.2795630

Crooker, N. U., Eastman, T. E., & Stiles, G. S. (1979). Observations of plasma depletion in the magnetosheath at the dayside magnetopause. *Journal of Geophysical Research*, *84*(A3), 869–874. https://doi.org/10.1029/JA084iA03p00869

Genestreti, K. J., Burch, J. L., Cassak, P. A., Torbert, R. B., Ergun, R. E., Varsani, A., et al. (2017). The effect of a guide field on local energy conversion during asymmetric magnetic reconnection: MMS observations. *Journal of Geophysical Research: Space Physics*, *122*, 11,342–11,353. https://doi.org/10.1002/2017JA024247

Haggerty, C. C., Shay, M. A., Drake, J. F., Phan, T. D., & McHugh, C. T. (2015). The competition of electron and ion heating during magnetic reconnection. *Geophysical Research Letters*, *42*, 9657–9665. https://doi.org/10.1002/2015GL065961

Hasegawa, H., Wang, J., Dunlop, M. W., Pu, Z. Y., Zhang, Q. H., Lavraud, B., et al. (2010). Evidence for a flux transfer event generated by multiple X-line reconnection at the magnetopause. *Geophysical Research Letters*, *37*, L16101. https://doi.org/10.11029/12010GL044219

Hesse, M., Birn, J., & Schindler, K. (1990). On the topology of flux transfer events. *Journal of Geophysical Research*, *95*(A5), 6549–6560. https://doi.org/10.1029/JA095iA05p06549

Kacem, I., Jacquey, C., Génot, V., Lavraud, B., Vernisse, Y., Marchaudon, A., et al. (2018). Magnetic reconnection at a thin current sheet separating two interlaced flux tubes at the Earth's magnetopause. *Journal of Geophysical Research: Space Physics*, *123*, 1779–1793. https://doi.org/10.1002/2017JA024537

Lee, L. C., Ma, Z. W., Fu, Z. F., & Otto, A. (1993). Topology of magnetic flux ropes and formation of fossil flux transfer events and boundary layer plasmas. *Journal of Geophysical Research*, *98*(A3), 3943–3951. https://doi.org/10.1029/92JA02203

Louarn, P., Fedorov, A., Budnik, E., Fruit, G., Sauvaud, J. A., Harvey, C. C., et al. (2004). Cluster observations of complex 3D magnetic structures at the magnetopause. *Geophysical Research Letters*, *31*, L19805. https://doi.org/10.1029/2004GL020625

Nishida, A. (1989). Can random reconnection on the magnetopause produce the low latitude boundary layer? *Geophysical Research Letters*, *16*, 227–230. https://doi.org/10.1029/GL016i003p00227

Øieroset, M., Phan, T. D., Eastwood, J. P., Fujimoto, M., Daughton, W., Shay, M. A., et al. (2011). Direct evidence for a three-dimensional magnetic flux rope flanked by two active magnetic reconnection X lines at Earth's magnetopause. *Physical Reviews Letters*, *107*(16). https://doi.org/10.1103/PhysRevLett.107.165007

Øieroset, M., Phan, T. D., Haggerty, C., Shay, M. A., Eastwood, J. P., Gershman, D. J., et al. (2016). MMS observations of large guide field symmetric reconnection between colliding reconnection jets at the center of a magnetic flux rope at the magnetopause. *Geophysical Research Letters*, *43*, 5536–5544. https://doi.org/10.1002/2016GL069166

Øieroset, M., Sundkvist, D., Chaston, C. C., Phan, T. D., Mozer, F. S., McFadden, J. P., et al. (2014). Observations of plasma waves in the colliding jet region of a magnetic flux rope flanked by two active X lines at the subsolar magnetopause. *Journal of Geophysical Research: Space Phyiscs*, *119*, 6256–6272. https://doi.org/10.1002/2014JA020124

Otto, A. (1995). Forced three-dimensional magnetic reconnection due to linkage of magnetic flux tubes. *Journal of Geophysical Research*, *100*(A7), 11,863–11,874. https://doi.org/10.1029/94JA03341

Paschmann, G., Haerendel, G., Papamastorakis, I., Sckopke, N., Bame, S. J., Gosling, J. T., & Russell, C. T. (1982). Plasma and magnetic field characteristics of magnetic flux transfer events. *Journal of Geophysical Research*, *87*(A4), 2159–2168. https://doi.org/10.1029/JA087iA04p02159

Paschmann, G., Øieroset, M., & Phan, T. (2013). In-situ observations of reconnection in space. *Space Science Reviews*, *178*, 385. https://doi.org/10.1007/s11214-012-9957-2

Paschmann, G., Sckopke, N., Haerendel, G., Papamastorakis, J., Bame, S. J., Asbridge, J. R., et al. (1978). ISEE plasma observations near the subsolar magnetopause. *Space Science Reviews*, *22*, 717. https://doi.org/10.1007/BF00212620

Perez, G. F., Cardoso, F. R., Sibeck, D., Gonzalez, W. D., Facskó, G., Coxon, J. C., & Pembroke, A. D. (2018). Generation mechanism for interlinked flux tubes on the magnetopause. *Journal of Geophysical Research: Space Physics*, *123*, 1337–1355. https://doi.org/10.1002/2017JA024664

Phan, T. D., Eastwood, J. P., Cassak, P. A., Øieroset, M., Gosling, J. T., Gershman, D. J., et al. (2016). MMS observations of electron-scale filamentary currents in the reconnection exhaust and near the X line. *Geophysical Research Letters*, *43*, 6060–6069. https://doi.org/10.1002/2016GL069212

Phan, T., Eastwood, J. P., Shay, M. A., Drake, J. F., Sonnerup, B. U. Ö., Fujimoto, M., et al. (2018). Electron magnetic reconnection without ion coupling in Earth's turbulent magnetosheath. *Nature*, *557*, 202–206. https://doi.org/10.1038/s41586-018-0091-5

Phan, T. D., Gosling, J. T., Paschmann, G., Pasma, C., Drake, J. F., Øieroset, M., et al. (2010). The dependence of magnetic reconnection on plasma β and magnetic shear: Evidence from solar wind observations. *Astrophysics Journal Letter*, *719*, L199. https://doi.org/10.1088/2041-8205/719/2/L199

Phan, T. D., Paschmann, G., Gosling, J. T., Oieroset, M., Fujimoto, M., Drake, J. F., & Angelopoulos, V. (2013). The dependence of magnetic reconnection on plasma β and magnetic shear: Evidence from magnetopause observations. *Geophysical Research Letters*, *40*, 11–16. https://doi.org/10.1029/2012GL054528

Phan, T. D., Shay, M. A., Gosling, J. T., Fujimoto, M., Drake, J. F., Paschmann, G., et al. (2013). Electron bulk heating in magnetic reconnection at Earth's magnetopause: Dependence on the inflow Alfvén speed and magnetic shear. *Geophysical Research Letters*, *40*, 4475–4480. https://doi.org/10.1002/grl.50917

Pollock, C., Moore, T., Jacques, A., Burch, J., Gliese, U., Saito, Y., et al. (2016). Fast plasma investigation for magnetospheric multiscale. *Space Science Reviews*, *199*(1-4), 331–406. https://doi.org/10.1007/s11214-016-0245-4

Russell, C. T., Anderson, B. J., Baumjohann, W., Bromund, K. R., Dearborn, D., Fischer, D., et al. (2014). The magnetospheric multiscale magnetometers. *Space Science Reviews*, *199*(1-4), 189–256. https://doi.org/10.1007/s11214-014-0057-3

Schwartz, S. J. (1998). Shock and discontinuity normals, Mach numbers and related parameters. In G. Paschmann & P. W. Daly (Eds.), *Analysis methods for multi-spacecraft data* (pp. 249–270). Bern: International Space Science Institute.

Shay, M. A., Drake, J. F., Denton, R. E., & Biskamp, D. (1998). Structure of the dissipation region during collisionless magnetic reconnection. *Journal of Geophysical Research*, *103*(A5), 9165–9176. https://doi.org/10.1029/97JA03528

Shay, M. A., Haggerty, C. C., Phan, T. D., Drake, J. F., Cassak, P. A., Wu, P., et al. (2014). Electron heating during magnetic reconnection: A simulation scaling study. *Physics of Plasmas*, *21*, 122902. https://doi.org/10.1063/1.4904203

Sonnerup, B. U., & Cahill, L. J. Jr. (1967). Magnetopause structure and attitude from Explorer 12 observations. *Journal of Geophysical Research*, *72*(1), 171–183. https://doi.org/10.1029/JZ072i001p00171

Sonnerup, B. U. Ö. (1979). Magnetic field reconnection. In L. T. Lanzerotti, C. F. Kennel, & E. N. Parker (Eds.), *Solar system plasma physics* (Vol. III, pp. 45–108). New York: North-Holland.

Swisdak, M., Opher, M., Drake, J. F., & Alouani Bibi, F. (2010). The vector direction of the interstellar magnetic field outside the heliosphere. *Astrophysics Journal*, *710*, 1769. https://doi.org/10.1088/0004-637X/710/2/1769

Swisdak, M., Rogers, B. N., Drake, J. F., & Shay, M. A. (2003). Diamagnetic suppression of component magnetic reconnection at the magnetopause. *Journal of Geophysical Research*, *108*(A5), 1218. https://doi.org/10.1029/2002JA009726

Torbert, R. B., Russell, C. T., Magnes, W., Ergun, R. E., Lindqvist, P. A., LeContel, O., et al. (2014). The FIELDS instrument suite on MMS: Scientific objectives, measurements, and data products. *Space Science Reviews*, *199*(1-4), 105–135. https://doi.org/10.1007/s11214-014-0109-8

Wilder, F. D., Ergun, R. E., Eriksson, S., Phan, T. D., Burch, J. L., Ahmadi, N., et al. (2017). Multipoint measurements of the electron jet of symmetric magnetic reconnection with a moderate guide field. *Physical Review Letters*, *118*, 265101. https://doi.org/10.1103/PhysRevLett.118.265101